Technical Memorandum ERL WPL-202

FREQUENCY CORRELATION OF ATMOSPHERIC SCINTILLATION

James H. Churnside
Richard J. Lataitis
James J. Wilson

Wave Propagation Laboratory
Boulder, Colorado
July 1991

noaa NATIONAL OCEANIC AND ATMOSPHERIC ADMINISTRATION / Environmental Research Laboratories

NOAA Technical Memorandum ERL WPL-202

FREQUENCY CORRELATION OF ATMOSPHERIC SCINTILLATION

James H. Churnside
Richard J. Lataitis
James J. Wilson

Wave Propagation Laboratory
Boulder, Colorado
July 1991

UNITED STATES
DEPARTMENT OF COMMERCE

Robert A. Mosbacher
Secretary

NATIONAL OCEANIC AND
ATMOSPHERIC ADMINISTRATION

John A. Knauss
Under Secretary for Oceans
and Atmosphere/Administrator

Environmental Research
Laboratories

Joseph O. Fletcher
Director

NOTICE

Mention of a commercial company or product does not constitute an endorsement by NOAA/ERL. Use of information from this publication concerning proprietary products or the tests of such products for publicity or advertising purposes is not authorized.

For sale by the National Technical Information Service, 5285 Port Royal Road
Springfield, VA 22161

Contents

Frequency Correlation of Atmospheric Scintillation

James H. Churnside, Richard J. Lataitis, and James J. Wilson

ABSTRACT. We present the results of measurements of the correlation of scintillations of two colors of light made in the turbulent atmosphere. In strong path-integrated turbulence, the correlation is below that predicted by the weak-turbulence theory. A simple theoretical approximation is used to account for saturation effects. This simple theory provides a reasonable approximation to the data. Thus, we conclude that saturation effects reduce the frequency correlation of atmospheric scintillation.

1. INTRODUCTION

The problem of spectral correlation of optical propagation through the turbulent atmosphere has been studied for some time. Early work, motivated by stellar scintillation, used the method of smooth perturbations to calculate the correlation for plane-wave propagation.[1-3] This same method was later applied to spherical-wave propagation.[4] A similar approach was used to calculate the log-amplitude correlation under various propagation geometries.[5-7]

Gurvich et al.[8] measured the two-frequency correlation in strong path-integrated turbulence, where the method of smooth perturbations and related methods are not valid. Zavorotnyi[9] developed an asymptotic expression for the correlation function, but this did not agree very well with the data. Much stronger path-integrated turbulence during the experiment would probably have resulted in better agreement.

The effect of a finite aperture on spectral correlation has also been considered. A theoretical expression was developed for weak path-integrated turbulence.[10] For strong path-integrated turbulence, the investigation was experimental.[11] No comparison of the theory and experiment was attempted because of the differences in conditions. Ben-Yosef et al.[12] conducted an experiment over a wider range of experimental conditions, and compared the results to the weak path-integrated turbulence theory. They postulated an inner-scale effect to explain their data, although this could not be checked because inner scale was not measured in the experiment.

In this paper, we present data with similarly low correlation values. Simultaneous measurements of inner scale show that the postulated inner-scale effect is not present. A simple theory of saturation is presented that shows that the reduced correlation is probably because of saturation effects.

2. THEORY

The bichromatic covariance of the normalized irradiance fluctuations I_1 and I_2 from two spherical waves at wavelengths λ_1 and λ_2, respectively, as observed through an incoherent receiver with a uniform circular aperture of diameter D, is given by[13]

$$B_{1,2}(\lambda_1, \lambda_2, D, l_o) = 16\,\pi^2 k_1 k_2 \int_o^L dz \int_o^\infty dK\, K\, \Phi_n\left[K, C_n^2(z), l_o(z)\right] \tag{1}$$

$$\sin\left[\frac{K^2 z(L-z)}{2k_1 L}\right] \sin\left[\frac{K^2 z(L-z)}{2k_2 L}\right] \left[2\frac{J_1(KDz/2L)}{(KDz/2L)}\right],$$

where $k_{1,2} = 2\pi/\lambda_{1,2}$ is the optical wavenumber, L is the propagation path length, z is the position along the path of a refractive irregularity with transverse wavenumber K, and Φ_n is the three-dimensional spectral density of the refractive index fluctuations. The refractive index power spectrum Φ_n is assumed to be isotropic. Its dependence on the refractive index structure parameter C_n^2, which describes the level of the spectrum, and on the inner scale l_o, which characterizes the high wavenumber cutoff of the spectrum, is explicitly shown. Outer-scale effects are not included because of the dominance of the smaller-scale refractive irregularities in producing the observed irradiance fluctuations. The effects of dispersion are also neglected.[13] Equation (1) is valid only in weak turbulence when the corresponding monochromatic variances $\sigma_1^2 = B_{1,2}(\lambda_1, \lambda_1, D, l_o)$ and $\sigma_2^2 = B_{1,2}(\lambda_2, \lambda_2, D, l_o)$ satisfy $\sigma_1^2, \sigma_2^2 < 1$.

Several forms for the refractive index spectrum Φ_n can be used in Eq. (1). We consider only those that can be expressed as the product of the Kolmogorov spectrum[14] Φ_K and a function F_{IS}, which describes the high wavenumber cutoff of the spectrum associated with the inner scale. To this end we write

$$\Phi_n\left[K, C_n^2(z), l_o(z)\right] = \Phi_K\left[K, C_n^2(z)\right] F_{IS}\left[K, l_o(z)\right], \tag{2a}$$

and

$$\Phi_K\left[K, C_n^2(z)\right] = 0.033 C_n^2(z) K^{-11/3}, \tag{2b}$$

where F_{IS} can be any of a number of functions, including a Gaussian form proposed by Tatarskii,[14] an exact numerical solution to the governing second-order linear homogeneous differential equation calculated by Hill,[15] or a corresponding analytical approximation proposed by Churnside.[16] We use the last in our calculations, given by

$$F_{IS}\left[K, l_o\right] = \exp\left(-1.28K^2 l_o^2\right) + 1.45\exp\left\{-0.97\left[\ln(Kl_o) - 0.45\right]^2\right\}. \tag{2c}$$

Equation (1) can be written in the following form, which makes the effect of a nonzero inner scale and aperture diameter on the corresponding bichromatic correlation coefficient R =

$B_{1,2}/\sqrt{\sigma_1^2\,\sigma_2^2}$ more transparent:

$$B_{1,2}(\lambda_1, \lambda_2, D, l_o) = 0.033\,\frac{4\pi^2}{L^2}\int_o^L dz\, C_n^2(z)\, z^2 (L - z)^2$$

$$\int_o^\infty dK\, K^{4/3}\, F_{IS}[K, l_o(z)]\, F_{FZ_1}\left(K, \sqrt{\lambda_1 L}\right) F_{FZ_2}\left(K, \sqrt{\lambda_2 L}\right) F_A(K, D), \tag{3a}$$

where we have used Eqs. (2a) and (2b),

$$F_{FZ_{1,2}}\left(K, \sqrt{\lambda_{1,2} L}\right) = \mathrm{sinc}\left[\frac{K^2 z(L-z)}{2k_{1,2}}\right], \tag{3b}$$

$$F_A(K, D) = J_{1c}\left(\frac{KDz}{2L}\right), \tag{3c}$$

$\mathrm{sinc}(x) = \sin(x)/x$ and $J_{1c}(x) = 2J_1(x)/x$. Note all the functions $F(K, \Lambda_c)$ that appear in Eq. (3) describe low-pass wavenumber filters associated with the inner scale (IS), the Fresnel zones $\sqrt{\lambda_1 L}$ and $\sqrt{\lambda_2 L}$ (FZ_1 and FZ_2, respectively), and the aperture (A). These functions are unity below a cutoff wavenumber $K_c \approx 2\pi/\Lambda_c$ and tend to zero for $K >> K_c$. Clearly, the function with the lowest wavenumber cutoff K_c dominates the convergence of the K integral in Eq. (3a).

First consider the limit $l_o = D = 0$ (i.e., $F_{IS} = F_A = 1$) and $\lambda_1 = \lambda_2 = \lambda$ (i.e., $F_{FZ_1} = F_{FZ_2} = F_{FZ}$) for which the bichromatic cross-covariance $B_{1,2} = \sigma_1^2 = \sigma_2^2$ and $R = 1$. In this limit, the function F_{FZ}^2 dominates the convergence of the K integral by introducing a cutoff at wavenumber $K_{FZ} \approx 2\pi/\sqrt{\lambda L}$. Now consider the limit $l_o = D = 0$ and $\lambda_1 > \lambda_2$. The functions F_{FZ_1} and $F_{FZ_1}^2$, corresponding to the longer wavelength λ_1, dominate the convergence of the K integral associated with the expressions for $B_{1,2}$ and σ_1^2, respectively. Both functions have a cutoff $K_{FZ_1} \approx 2\pi/\sqrt{\lambda_1 L}$, so that to a good approximation, $B_{1,2} \approx \sigma_1^2$. The convergence of the K integral associated with the expression for σ_2^2 is dominated by the function $F_{FZ_2}^2$, which has a cutoff $K_{FZ_1} \approx 2\pi/\sqrt{\lambda_1 L}$ that is greater than the cutoff for F_{FZ_1}. Therefore we expect $\sigma_2^2 > \sigma_1^2$ and $R < 1$.

To examine the effect of a nonzero inner scale, we consider the limit $D = 0$ (i.e., $F_A = 1$) and $\lambda_1 > \lambda_2$. The function F_{IS} introduces a wavenumber cutoff at $K_{IS} \approx 2\pi/l_o$ that affects the convergence of the K integral associated with the expressions for $B_{1,2}$ and σ_1^2 only when $l_o > \sqrt{\lambda_1 L}$. For this case we still have $B_{1,2} \approx \sigma_1^2$, as in the limit $l_o = 0$, though the individual values of $B_{1,2}$

and σ_1^2 have been proportionally reduced because of the lower wavenumber cutoff associated with F_{IS} when compared to that for F_{FZ_1}. The inner-scale cutoff associated with the function F_{IS} in the corresponding expression for σ_2^2 also dominates the corresponding K integration when $l_o > \sqrt{\lambda_1 L}$ because we have assumed $\lambda_1 > \lambda_2$. In this limit, $\sigma_2^2 \approx \sigma_1^2 \approx B_{1,2}$ are all independent of wavelength and $R \approx 1$. Therefore the bichromatic correlation coefficient R tends to unity for inner scales that are larger than the larger Fresnel zone (i.e., $l_o > \sqrt{\lambda_1 L}$). This is equivalent to the well-known result that geometric optics is valid when the inner scale is large since geometric optics implies no wavelength dependence. An identical argument for the effect of a finite aperture shows that R tends to unity for aperture diameters D that are larger than the larger Fresnel zone (i.e., $D > \sqrt{\lambda_1 L}$). We also note that for inner scales comparable to or larger than the larger Fresnel zone, aperture effects will become evident only when $D > l_o$, and will further increase the correlation between the fluctuating irradiances.

To numerically investigate inner-scale and aperture effects on the bichromatic correlation coefficient R, we assume uniform turbulence so that C_n^2 and l_o are independent of position along the path. We make the variable transformations $u = z/L$ and $x = K[L(\lambda_1 + \lambda_2)/2]^{1/2}$. If we also define $\Delta = |\lambda_1 - \lambda_2|/(\lambda_1 + \lambda_2)$, $\alpha = l_o\,[L(\lambda_1 + \lambda_2)/2]^{-1/2}$, and $\beta = D\,[L(\lambda_1 + \lambda_2)/2]^{-1/2}$, we can write

$$R(\alpha, \beta, \Delta) = (1-\Delta^2)^{-5/12} \frac{G(\alpha, \beta, \Delta)}{\left[G\left(\frac{\alpha}{\sqrt{1+\Delta}}, \frac{\beta}{\sqrt{1+\Delta}}, 0\right) G\left(\frac{\alpha}{\sqrt{1-\Delta}}, \frac{\beta}{\sqrt{1-\Delta}}, 0\right)\right]^{1/2}} \tag{4a}$$

where

$$G(\alpha, \beta, \Delta) = \int_0^1 du \int_0^\infty dx\, x^{-8/3}\, F_{IS}(\alpha x) \times \sin\left[\frac{1}{4\pi}(1-\Delta)u(1-u)x^2\right] \sin\left[\frac{1}{4\pi}(1+\Delta)u(1-u)x^2\right] \times 2\,\frac{J_1\left(\frac{1}{2}\beta u x\right)}{\frac{1}{2}\beta u x} \tag{4b}$$

and $F_{IS}(\alpha x)$ is defined by Eq. (2c).

Note that the bichromatic correlation coefficient depends only on α, β, and Δ. For a point receiver and a medium with zero inner scale, β and α are both zero, and Eq. 4 reduces to[12]

$$R(0, 0, \Delta) = \frac{1 - \Delta^{5/6}}{(1 - \Delta^2)^{5/12}} . \qquad (5)$$

For nonzero inner scale, the correlation coefficient is higher. Figure 1 is a plot of the correlation coefficient for a point receiver with nonzero inner scale for $\Delta = 0.178$ ($\lambda_1 = 0.633$ μm and $\lambda_2 = 0.442$ μm) and for $\Delta = 1/3$ ($\lambda_2 = \lambda_1/2$). In both cases, the correlation coefficient increases from the value of Eq. (5) for small inner scale to unity at large inner scale. The minimum correlation in each curve is due to the bump in the turbulent spectrum near the inner scale. The differences at the two wavelengths are enhanced when this bump coincides with the average Fresnel zone size.

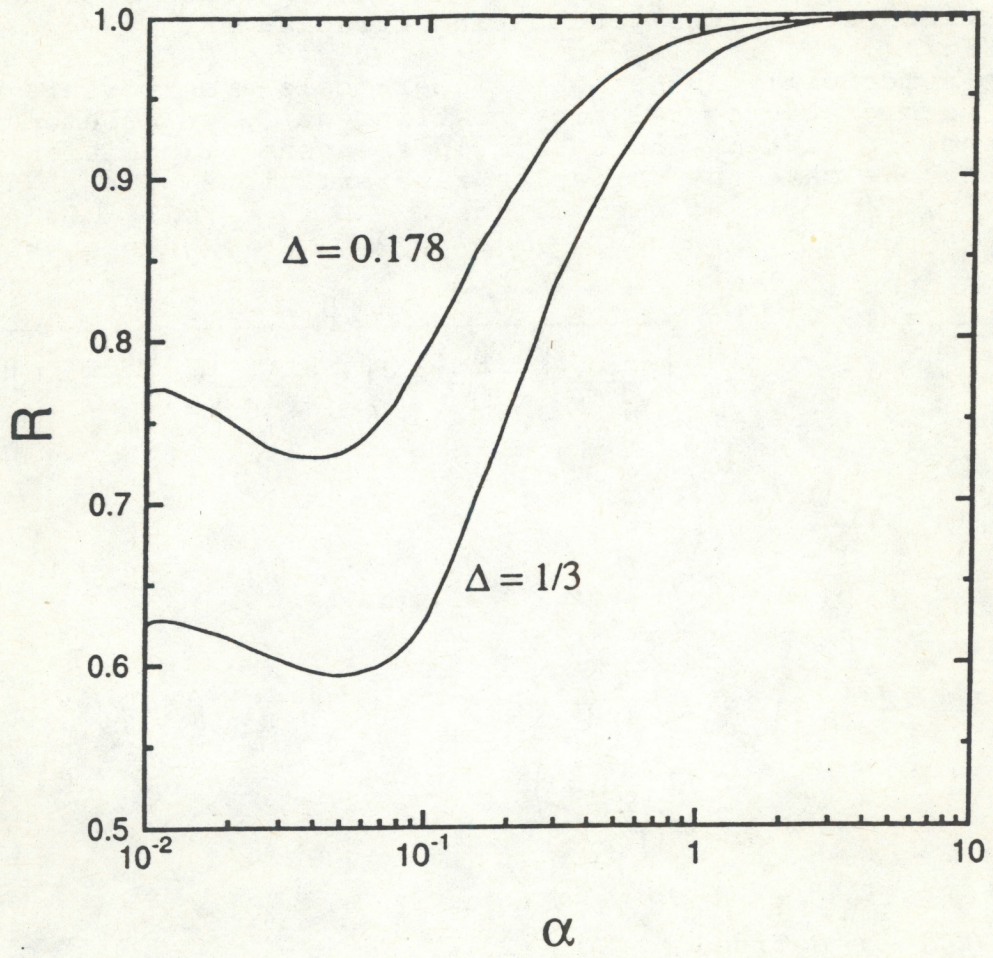

Figure 1. Correlation coefficient R as a function of inner-scale parameter α for a point receiver and for two values of wavelength separation Δ.

The correlation coefficient is also higher for a nonzero aperture diameter. This is shown in Fig. 2, where the correlation coefficient increases to unity as the aperture diameter increases. Only the case of $\Delta = 0.178$ is shown, but curves are plotted for several values of α.

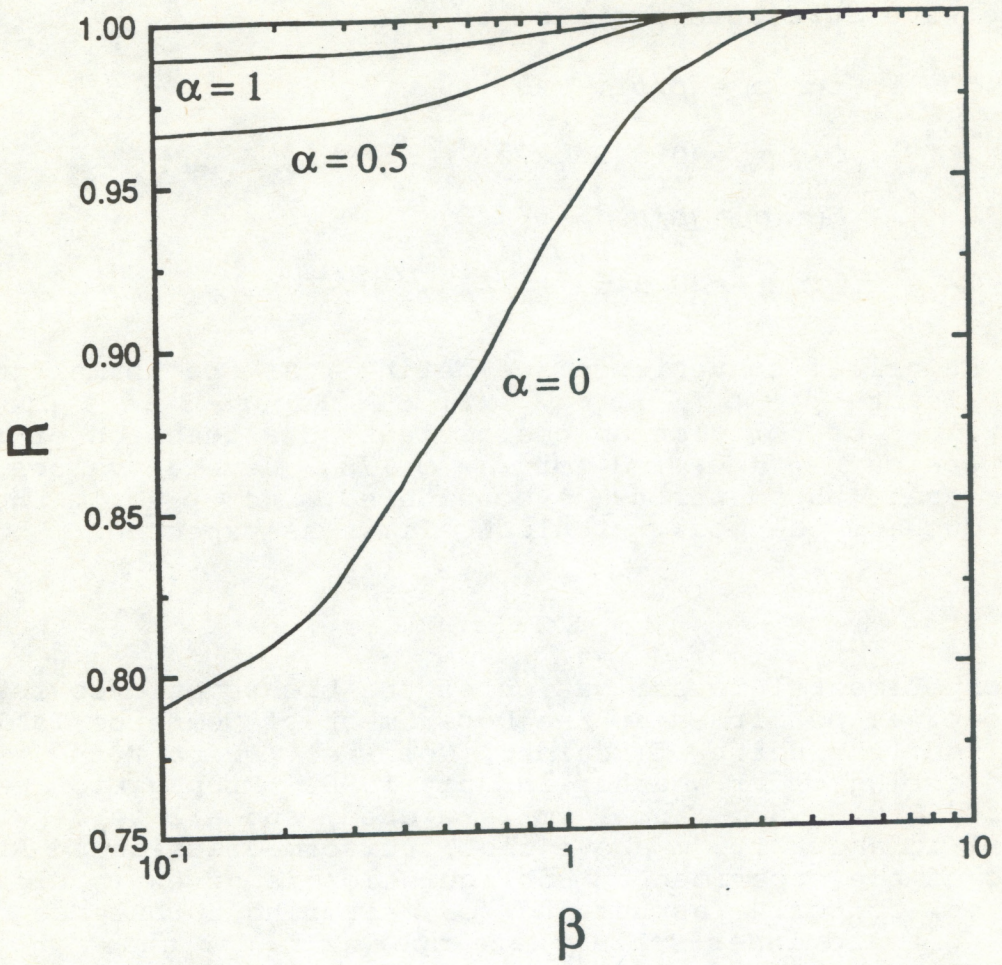

Figure 2. Correlation coefficient R as a function of aperture size parameter β for several values of inner scale parameter α and for wavelength separation of $\Delta = 0.178$.

For strong path-integrated turbulence, we postulate another filter function within the integrals of Eq. (1). There is no rigorous theoretical justification for this postulate. We note that the effectiveness of eddies larger than the transverse wave coherence length ρ_o is reduced because of the loss of coherence of the incident field. Thus, we consider a filter function given by the mutual coherence function (MCF) of the field at path position z and at a separation given by $2/K$. This seems

physically reasonable and describes the data fairly well without introducing adjustable parameters.

The MCF is given by

$$\text{MCF} = \exp\left[-\frac{1}{2}D(z, 2/K)\right], \tag{6}$$

where the wave structure function is

$$D(z, p) = (p/\rho_o)^{5/3} \quad \text{for } \rho_o = \left(0.545 k_1 k_2 z C_n^2\right)^{-3/5} >> l_o \tag{7a}$$

$$D(z, p) = (p/\rho_o)^2 \quad \text{for } \rho_o = \left(0.545 k_1 k_2 z C_n^2 l_o^{-1/3}\right)^{-1/2} << l_o. \tag{7b}$$

For numerical convenience, we define ρ as the normalized coherence length $\rho = \rho_o[L(\lambda_1 + \lambda_2)/2]^{-1/2}$. Figure 3 is a plot of typical values of correlation coefficient as a function of ρ for a point receiver ($\beta = 0$) and for $\Delta = 0.178$. Several values of the inner-scale parameter α are considered. For $\rho >> 1$, the values reduce to the weak turbulence limit as expected.

3. EXPERIMENT

An experimental investigation of the bichromatic correlation coefficient was performed at the Department of Commerce Table Mountain facility north of Boulder, Colorado. Data were collected during clear weather in July 1990. Propagation paths of 100 m, 250 m, 500 m, and 1 km were used, and all were horizontal at about 1.5 m above flat, uniform grassland. A schematic of the experimental configuration is given in Fig. 4. In addition, optical instruments for measuring turbulence strength C_n^2 [17] and inner scale[18] were operated near the propagation paths during the experiment.

The transmitter comprises two lasers: a 10-mW He-Ne with a wavelength of 633 nm and a 20-mW He-Cd with a wavelength of 442 nm. The beams from the two lasers are combined with a dichroic beamsplitter. A diverging lens was used to expand the beams; a different lens was used at each path length to maintain a spot diameter of about 1 m at the receiver. A radio-controlled shutter was placed in front of the transmitter to allow the background light level to be periodically measured.

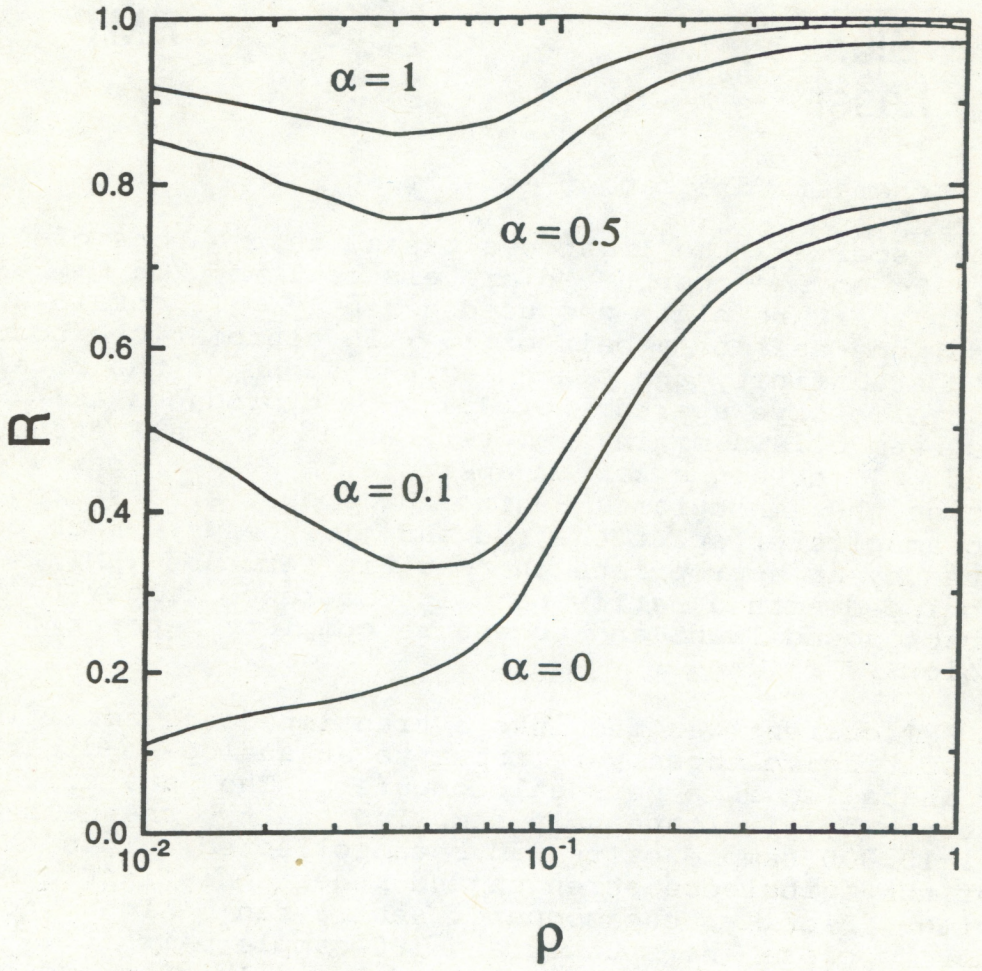

Figure 3. Correlation coefficient R as a function of coherence length parameter ρ for several values of inner-scale parameter α with wavelength separation $\Delta = 0.178$ and aperture parameter $\beta = 0$.

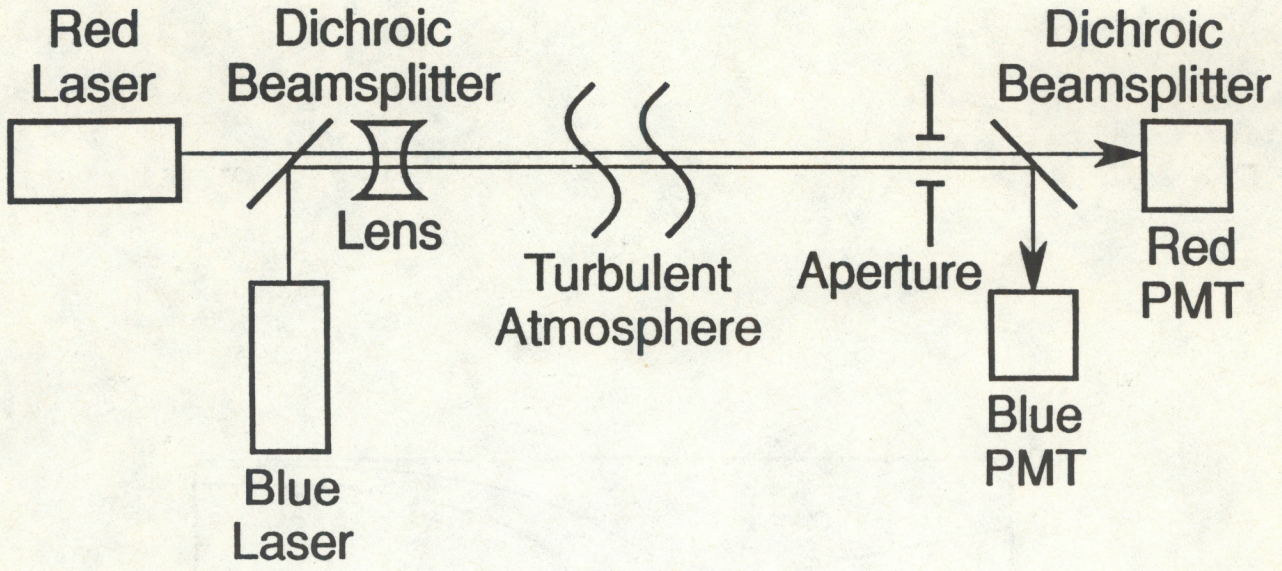

Figure 4. Schematic diagram of experiment.

At the receiver, the light was passed through one of six apertures. To obtain aperture diameters of 1 mm, 2.5 mm, 5 mm, and 1 cm, an aperture plate was used directly. To obtain a 4.4-cm aperture, one-half of a pair of 10 × 50 achromatic binoculars was focused at infinity and placed at the front of the receiver. This has an effective aperture of 4.4 cm and produces a collimated beam of 4.4 mm in diameter, which is small enough to be detected. To obtain a 2.5-cm aperture, a 2.5-mm aperture was placed behind the binocular. Behind the aperture, a second dichroic beamsplitter split the red and blue beams. Each beam was detected by an appropriate photomultiplier tube (PMT). Each PMT was equipped with a narrow band interference filter to minimize background light and to ensure complete separation of the two colors.

Each PMT current was fed into a transimpedance amplifier, and the resulting voltages were input to an analog-to-digital converter installed in a personal computer. The data collection sequence began by simultaneously sampling the two channels every 2 ms until 10,000 sample pairs had been collected. Then the outputs of the turbulence strength and inner-scale instruments were sampled. Finally, the computer sent a radio signal to the transmitter to close the shutter and 300 sample pairs of background data were collected. This data collection cycle was repeated 25 times for each combination of path length and aperture diameter.

4. RESULTS

Before processing the data, the noise characteristics of each PMT were measured using a constant, incoherent light source. Both were found to be very nearly shot noise limited, with a

noise variance proportional to the output level. The measured proportionality constants were used to perform a statistical correction to the measured variances and covariance. All values reported are the corrected values.

Before presenting correlation data, it is instructive to plot the blue variance σ_b^2 as a function of the red variance σ_r^2 for the 1-mm-diameter aperture data. This is done in Fig. 5. We see that the 100 m data and the 250 m data are near the line $\sigma_b^2 = (\lambda_b/\lambda_r)^{7/6}\sigma_p^2$. This is true even though the variances at 250 m are too large for the weak-turbulence approximation to be strictly valid. As the path length increases, the blue wavelength reaches saturation first and the variance is reduced more than that of the red wavelength. For the 1-km path, the variances are nearly evenly scattered about the line $\sigma_b^2 = \sigma_r^2$. Note also that the scatter in the data becomes greater at longer path lengths. This suggests that the correlation coefficient is decreasing since the data must be along a straight line for unity correlation.

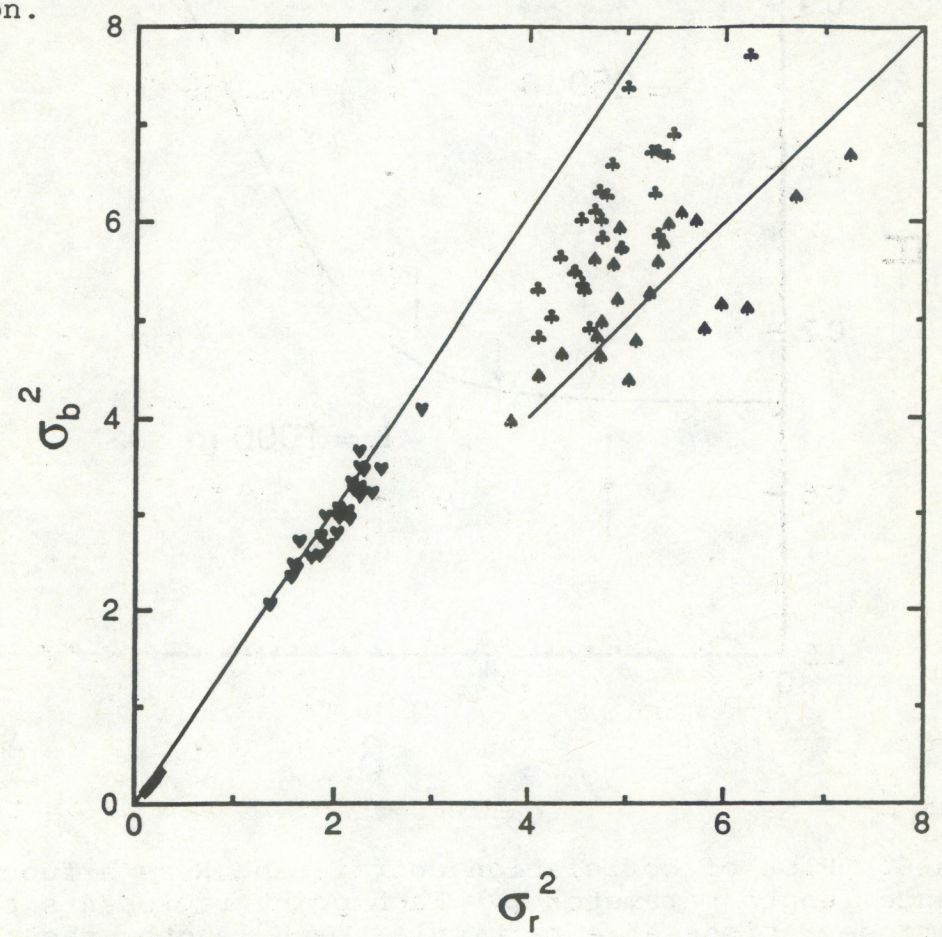

Figure 5. Plot of blue variance σ_b^2 as a function of red variance σ_r^2 for 100 m path (diamonds), 250 m path (hearts), 500 m path (clubs), and 1 km path (spades). Upper line is weak turbulence theoretical prediction $\sigma_b^2 = (\lambda_b/\lambda_r)^{7/6}\,\sigma_r^2$ and lower line is $\sigma_b^2 = \sigma_r^2$.

Figure 6 is a plot of correlation as a function of the coherence parameter ρ for the 1-mm aperture. The points represent the data from the four path lengths. The error bars represent the standard deviation of the 25 individual correlation values and the standard deviation of the 25 coherence parameter values calculated from individual C_n^2 and l_o values. The solid line was calculated using the theory with the MCF saturation filter. During the time the data were collected, C_n^2 was about 2×10^{-12} $m^{-2/3}$ and the inner scale was about 8 mm. For these values, $\alpha = 1.56\rho^{1/2}$. With the 1-mm aperture, $\beta = \alpha/8$. These values were used in the theoretical curve in Fig. 6.

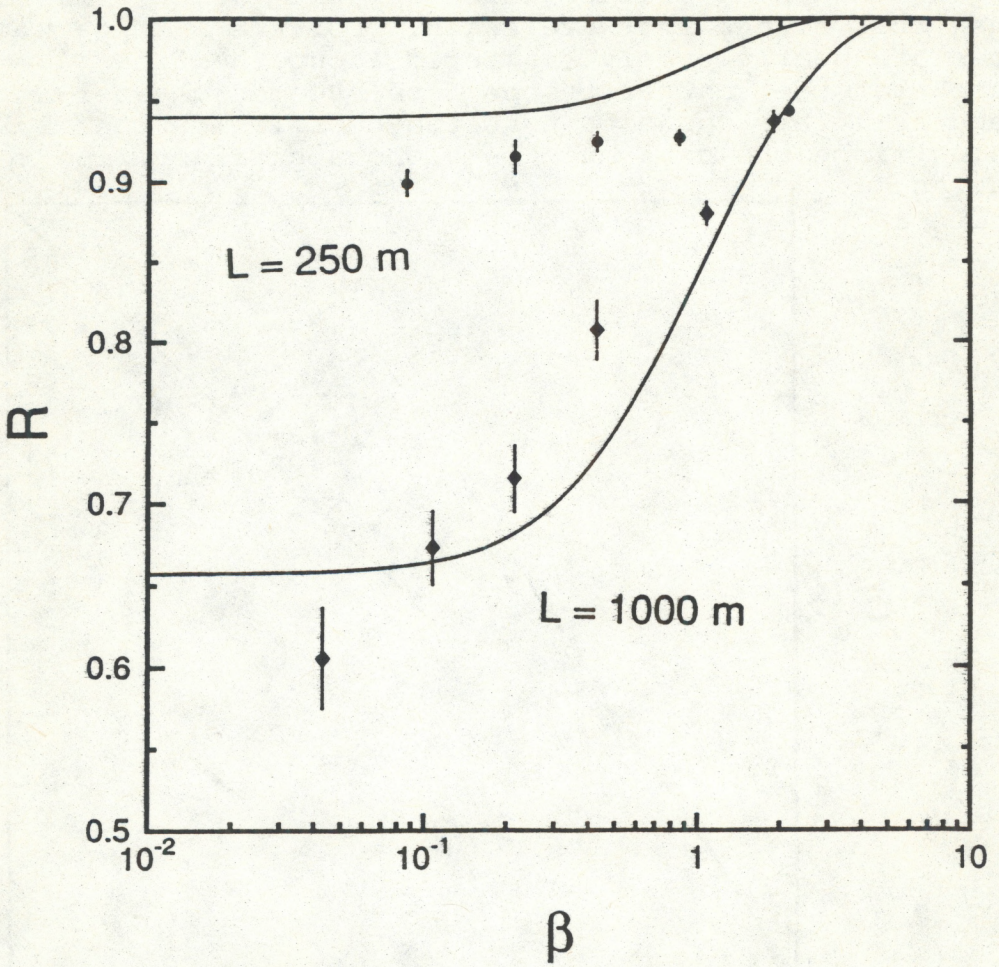

Figure 6. Plot of correlation coefficient R as a function of coherence length parameter ρ. Each point represents the mean and standard deviations at a particular path length, the solid line is the saturation theory, and the dashed line is the weak-turbulence theory.

The dashed line in Fig. 6 was calculated in the same manner, but neglecting saturation effects, and it is thus a weak-turbulence calculation. Although it is plotted as a function of ρ to allow comparison with the data, it should be thought of as a function of α and plotted against $\rho = 0.41\alpha^2$. We see that the weak turbulence theory is a very poor description of the data. Adding the MCF as a filter function improves the agreement.

Although direct comparison is impossible, these data are in general agreement with the plane-wave case of Zavorotnyi.[9] He uses the asymptotic theory to obtain a plane-wave correlation for the same wavelength separation of 0.43. The data value at the highest reported turbulence level is 0.55, which is similar to our long-path value of 0.61.

Figure 7 is a plot of the correlation as a function of aperture diameter parameter β for the 1000-m and 250-m paths. The agreement with the saturation theory is fairly good. One discrepancy between the data and the theory is apparent. The theory makes a quicker transition from the point-detector value to unity than the data. This is probably because the theory still uses the weak-turbulence aperture filter that assumes a single scale size at the Fresnel zone. At larger turbulence levels, a scintillation pattern contains two spatial scales. One of these, at the phase coherence length, is smaller than the Fresnel zone, and the other, at the scattering disk size, is larger than the Fresnel zone. This scale splitting may extend the transition region. Despite this, the simple theory proposed here seems to describe the data fairly accurately.

Acknowledgements

The authors thank Raymond Harrison for the data collection and processing software. This work was partially supported by the U.S. Army Atmospheric Sciences Laboratory under military interdepartmental purchase request ASL 90-8042.

References

1. V.I. Tatarskii, and L.N. Zhukova, On the chromatic scintillation of stars, *Dok. Acad. Nauk SSSR* 124, 567-570 (1959).

2. V.A. Zverev, Dispersive properties of media containing random inhomogeneities, *Radiophys. Quant. Electron.* 3, 371-373 (1960).

3. Y.A. Ryzhov and E.P. Lapteva, The fluctuations in the parameters of a triharmonic wave propagated through a locally-homogeneous medium, *Radiophys. Quant. Electron.* 3, 125-139 (1960).

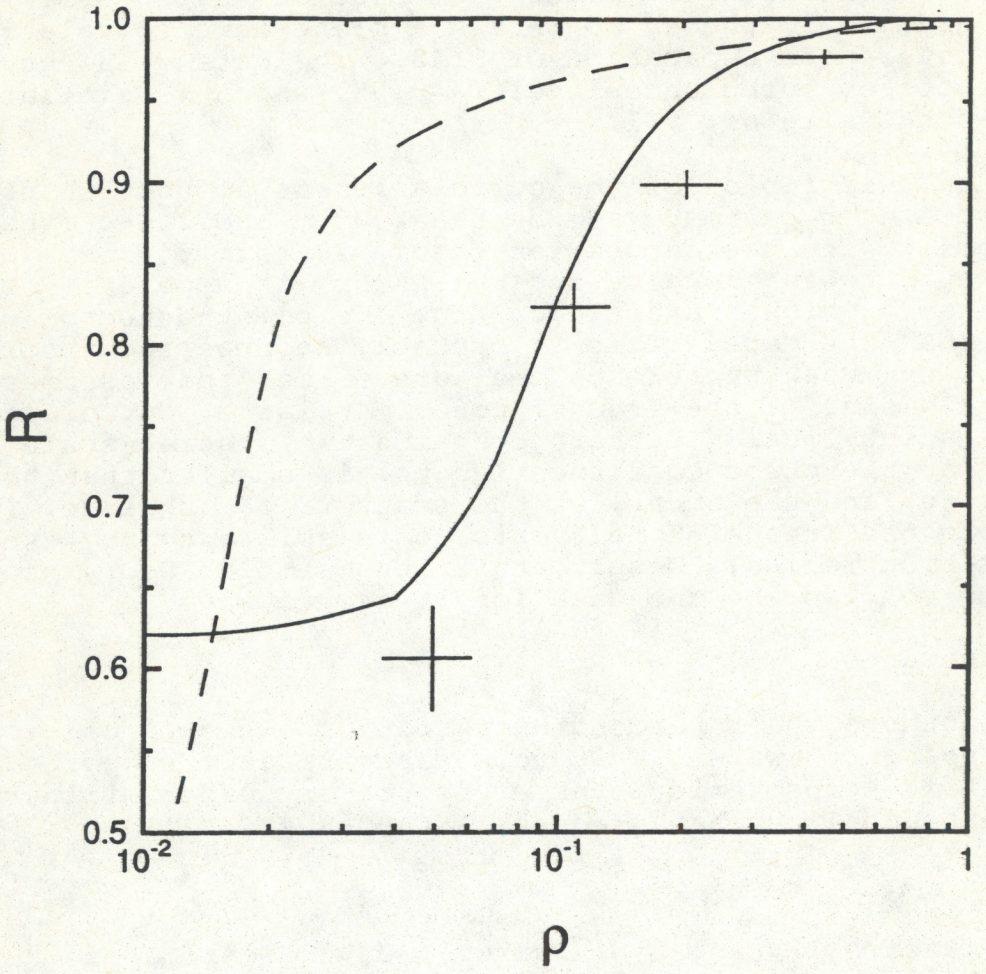

Figure 7. Plot of correlation coefficient as a function of aperture parameter β for two values of path length L.

4. I.M. Fuks, Correlation of the fluctuations of frequency-spaced signals in a randomly inhomogeneous medium, *Radiophys. Quant. Electron.* 17, 1272-1276 (1974).

5. A. Ishimaru, Temporal frequency spectra of multifrequency waves in turbulent atmosphere, *IEEE Trans. Antennas Propagat.* AP-20, 10-19 (1972).

6. A. Ishimaru, *Wave Propagation and Scattering in Random Media* (Academic Press, New York, 1978), vol. 2, p. 401.

7. Y. Baykal and M.A. Plonus, Two-source, two-frequency spherical wave structure functions in atmospheric turbulence, *J. Opt. Soc. Am.* 70, 1278-1279 (1980).

8. A.S. Gurvich, V. Kan, and Vl.V. Pokasov, Two-frequency fluctuations of light intensity in a turbulent medium, *Opt. Acta.* 26, 555-562 (1979).

9. V.U. Zavorotnyi, Frequency correlation of large intensity fluctuations in a turbulent medium, *Radiophys. Quant. Electron.* 24, 407-412 (1981).

10. M. Tamir, E. Azoulay, S. Tsur, and U. Halavee, Aperture-averaged spectral correlations of beams in a turbulent atmosphere, *Appl. Opt.* 23, 2359-2362 (1984).

11. Z. Azar, H.M. Loebenstein, G. Appelbaum, E. Azoulay, U. Halavee, M. Tamir, and M. Tur, Aperture averaging of the two-wavelength intensity covariance function in atmospheric turbulence, *Appl. Opt.* 24, 2401-2407 (1985).

12. N. Ben-Yosef, E. Goldner, and A. Weitz, Two-color correlation of scintillations, *Appl. Opt.* 25, 3486-3489 (1986).

13. R.J. Hill, and R.J. Lataitis, Effect of refractive dispersion on the bichromatic correlation of irradiances for atmospheric scintillation, *Appl. Opt.* 28, 4121-4125 (1989).

14. V.I. Tatarskii, *The Effects of the Turbulent Atmosphere on Wave Propagation* (Israel Program for Scientific Translations, Jerusalem, 1971).

15. R.J. Hill, Models of the scalar spectrum for turbulent advection, *J. Fluid Mech.* 88, 541-562 (1978).

16. J.H. Churnside, A spectrum of refractive turbulence in the turbulent atmosphere, *J. Mod. Opt.* 37, 13-16 (1990).

17. G.R. Ochs, W.D. Cartwright, and D.D. Russell, Optical C_n^2 Instrument Model II, NOAA Tech. Memo. ERL WPL-51 (available from National Technical Information Service, 5285 Port Royal Rd., Springfield, VA, 22161; order number WPL51:PB 80-209000), 1979.

18. G.R. Ochs, and R.J. Hill, Optical-scintillation method of measuring turbulence inner scale, *Appl. Opt.* 24, 2430-2432 (1979).

☆U.S. GOVERNMENT PRINTING OFFICE: 1991 - 573-002/21076